Greenhouse gas emissions from marine decommissioned hydrocarbon wells: leakage detection, monitoring and mitigation strategies

Christoph Böttner[a,*], Matthias Haeckel[a], Mark Schmidt[a], Christian Berndt[a], Lisa Vielstädte[a], Jakob A. Kutsch[b], Jens Karstens[a], Tim Weiß[a]

[a] *GEOMAR Helmholtz Centre for Ocean Research Kiel, Kiel, Germany*
[b] *Christian-Albrechts-Universität zu Kiel, Kiel, Germany*

A B S T R A C T

Hydrocarbon gas emissions from with decommissioned wells are an underreported source of greenhouse gas emissions in oil and gas provinces. The associated emissions may partly counteract efforts to mitigate greenhouse gas emissions from fossil fuel infrastructure. We have developed an approach for assessing methane leakage from marine decommissioned wells based on a combination of existing regional industrial seismic and newly acquired hydroacoustic water column imaging data from the Central North Sea. Here, we present hydroacoustic data which show that 28 out of 43 investigated wells release gas from the seafloor into the water column. This gas release largely depends on the presence of shallow gas accumulations and their distance to the wells. The released gas is likely primarily biogenic methane from shallow sources. In the upper 1,000 m below the seabed, gas migration is likely focused along drilling-induced fractures around the borehole or through non-sealing barriers. Combining available direct measurements for methane release from marine decommissioned wells with our leakage analysis suggests that gas release from investigated decommissioned hydrocarbon wells is a major source of methane in the North Sea (0.9-3.7 [95% confidence interval = 0.7-4.2] kt yr^{-1} of CH_4 for 1,792 wells in the UK sector of the Central North Sea). This means hydrocarbon gas emissions associated with marine hydrocarbon wells are not significant for the global greenhouse gas budget, but have to be considered when compiling regional methane budgets.

1. Introduction

Hydrocarbon gas emissions from offshore wells have to be considered when compiling regional gas budgets, particularly for methane (CH_4), which is the second most important greenhouse gas after carbon dioxide (Ciais et al., 2013; Saunois et al., 2016). The impact of anthropogenic methane emissions on climate change receives increasing attention (Saunois et al., 2016) as societies attempt to transit from coal as primary energy source to gas and further on to renewables. While our understanding of carbon dioxide (CO_2) sources and sinks is reasonably well established (Global emissions 2008-2017: 9.4 ± 0.5 Gt C yr^{-1}; Le Quéré et al., 2018), estimates for the global methane budget still show large uncertainties both with attributing and quantifying methane emissions, as evidenced by the large discrepancies between top-down and bottom-up estimates of global sources and sinks (Global emissions 2003-2012 top-down: 0.558 [0.540-0.568] Gt CH_4 yr^{-1}, bottom-up: 0.736 [0.596-0.884] Gt CH_4 yr^{-1}, uncertainties are reported as [min-max] range; Saunois et al., 2016). Top-down approaches are based on

atmospheric inversion models and describe the quantification of atmospheric methane concentrations and subsequent attribution to the various sources and sinks (Ciais et al., 2013). Bottom-up estimates, as presented in the manuscript, are process-based models and rely on quantification of individual processes and subsequent calculations of atmospheric methane concentrations (Ciais et al., 2013). Methane emissions from the up- and down-stream natural oil and gas sectors are estimated to reach 0.079 [min-max range = 0.069-0.088] Gt CH_4 yr^{-1} representing about 65% of total fossil CH_4 emissions for the decade 2003-2012 (Saunois et al., 2016). Emissions of methane and other hydrocarbon gases from abandoned wells add to this part of the budget, e.g. in Pennsylvania, U.S.A., abandoned wells contribute 5-8% of the annual anthropogenic methane emissions (Kang et al., 2016), and thus partly counteract efforts to mitigate greenhouse gas emissions from fossil fuel infrastructure (Brandt et al., 2014; Vielstädte et al., 2017).

Measured methane emissions from decommissioned wells span two orders of magnitude with higher releases for marine wells in proximity of shallow gas accumulations, i.e. 1-19 t yr^{-1} of CH_4 (Vielstädte et al.,

2015) and lower releases for unplugged onshore wells in the proximity of coal areas, i.e. 0.5 t yr^{-1} of CH_4 (Kang et al., 2016). Well attributes, such as geographic location, age, drilling data (spud date), production and abandonment, may be used as proxies to assess the leakage propensity of wells (Vielstädte et al., 2015; Kang et al., 2016; Townsend-Small et al., 2016). As onshore wells show a correlation of leakage with well attributes, i.e. geographic location, age, and proximity to shallow gas accumulations (Kang et al., 2016) it is likely that similar attributes may be identified for offshore boreholes (i.e. Vielstädte et al., 2015). In offshore areas seismic data have been used to identify shallow gas accumulations in the subsurface and help define areas where leakage is more likely (White, 1975; Anstey, 2013; Karstens & Berndt, 2015; Marfurt & Alves, 2015). The combination of seismic data and information on the status of wells and their spatial distribution should allow to constrain leakage propensity and flow of hydrocarbon gases from drilled wells. However, basic information, such as the number of wells or their location, even in regions with a long history of oil and gas exploration and production, are often poorly documented (e.g. Kang et al., 2016; Townsend-Small et al., 2016).

Leakage of hydrocarbon gases from offshore wells may occur as a result of two main processes: First, leakage may occur through faulty, damaged or corroded well casings and/or annuli commonly referred to as "well integrity issues" (Celia & Bachu, 2003; Gasda et al., 2004; Vrålstad et al., 2019). Second, for shallow marine sediment, we also consider that fluid migration may occur along the outside of the well through drilling-induced fractures surrounding the well path (Harrison et al., 1954; Gurevich et al., 1993; Aadnøy & Bell, 1998; Kårstad & Aadnøy, 2008; Bohnhoff & Zoback; 2010; Osborn et al., 2011; Vielstädte et al., 2015, 2017, 2019). However, currently little quantitative data exist for leakage through drilling-induced fracture networks outside of the borehole, most information is related to blowout scenarios (e.g. Leifer & Judd, 2015; Landrø et al., 2019).

Here, we present an approach for assessing the propensity of leakage from boreholes based on existing regional three-dimensional seismic data. For this purpose, we analyze the conditions for gas leakage from hydrocarbon wells in the Central North Sea (Fig. 1). We constrain the amount of methane that is escaping from specific decommissioned hydrocarbon wells into the North Sea based on hydroacoustic water column imaging. We first present our results (Section 4) from the seismic data analyses and testing of these results against direct measurements of the water column by hydroacoustic methods. We evaluate these findings (Section 5) against different leakage scenarios and derive possible constraints. We combine these constraints to approximate the total methane release from wells covered by seismic data in the Central North Sea to compare them to previous findings of our working group. Furthermore, we formulate recommendations for future borehole placements and best practice for drilling and decommissioning of wells to avoid inadvertent gas release after abandonment. In addition, we provide the basis for recommendations for prolonged leakage monitoring after abandonment.

2. Gas leakage

2.1. Gas migration through the overburden

The transport of fluids through marine sediments is primarily governed by pressure and permeability contrasts (Berndt, 2005). In general, Darcy's law, a specific solution of the Navier-Stokes-equations, describes fluid flow through sedimentary basins (Whitaker, 1986). More specific, Darcy's law describes the transport of fluid phases through permeable beds from deeper strata towards the surface dependent on the permeability of rocks and the hydraulic head (Whitaker, 1986). Permeability is a rock property that describes how easily fluids may move through them. Three-dimensional (3D) seismic data show that subsurface permeability barriers often correlate with a wide range of anomalies, which can be related to focused fluid migration. Focused

fluid flow is primarily directed upwards and occurs, when pore pressure exceeds the combined least principal stress and tensile strength of the sediment and induces hydrofracturing (Hubbert & Willis, 1957). Pore pressure may not need to exceed the least principal stress to enable fluid flow, if flow is focused along fluid pathways that can be reactivated before pore fluid pressure reaches the level of the least compressive stress. Aside from the Mohr-Coulomb failure criterion, fluids may also start to move if the pore pressure overcomes the capillary entry pressure and capillary failure occurs (Clayton & Hay, 1994). Both types of seal bypass commonly occur in areas where the fluid pressure is increased, i.e. by compaction, rapid loading, hydrothermal activity, or diagenetic processes (Berndt, 2005).

In seismic data, direct hydrocarbon indicators (DHI) highlight areas in the subsurface, where a hydrocarbon phase exists. Hydrocarbon accumulations are often manifest as seismic amplitude anomalies. These amplitude anomalies include seismic attenuation, velocity pushdown, bright spots, seismic chimneys or pipes and flat spots (White, 1975; Anstey, 2013; Karstens & Berndt, 2015; Marfurt & Alves, 2015). Seismic attenuation describes the energy absorption of a seismic wave due to the presence of free gas and the subsequent amplitude dimming of underlying reflectors. Velocity pushdown is an apparent depression of seismic reflectors (in the time domain) due to the decrease of seismic velocities in the accumulated gas phase above the reflectors. Bright spots are high amplitude seismic reflections with reversed polarity (with respect to the seafloor) that indicate a change in pore space filling (White, 1975). Seismic chimneys or pipes are the seismic expression of vertical fluid conduits attributed to localized release of overpressure in the subsurface and manifest themselves in seismic data as circular, often chaotic amplitude anomalies with dimmed reflections and bright spots at different stratigraphic levels (Cartwright, 2007; Løseth et al., 2009; Andresen, 2012; Karstens & Berndt, 2015). Flat spots indicate a fluid contact (oil/gas, gas/water, oil/water) and manifest themselves in seismic data as horizontal (high-amplitude) reflections that cut dipping strata.

In the North Sea, vertical gas migration is typically attributed to (I) structure-controlled flow, i.e. along faults or fracture zones (Gurevich et al., 1993; Berndt et al., 2003; Cartwright, 2007), (II) vertical fluid conduits (Karstens & Berndt, 2015; Böttner et al., 2019), or (III) well paths, including the well paths themselves and the fractured surroundings (Gurevich et al., 1993; Nordbotten et al., 2004, 2005; Vielstädte et al., 2015, 2017). Once migration pathways have formed, they may remain conductive for further gas migration from deeper strata towards the surface for millions of years (Dumke et al., 2014).

2.2. Regulations and guidelines for well abandonment in the North Sea

Procedures for well decommissioning, including plugging and abandonment (P&A), largely depend on the geographic location of the wells (e.g. national/international jurisdiction, onshore/offshore environment) and the operator (Fig. 1). The procedures for well plugging and abandonment are similar for both onshore and offshore wells. The operator is normally required to remove the completion hardware and establish well barriers (Abshire et al., 2012). Well barriers are "envelopes of one or several dependent well barrier elements preventing fluids or gases from flowing unintentionally from one formation into another formation - or to the surface" (NORSOK-D-010, 2013). For example, operators are required to install cement plugs at specific depths across permeable layers, such as water-bearing zones or reservoirs (Abshire et al., 2012). These cement plugs protect the permeable layer against out- and inflow, but also shield a formation from pressure differences from above and below. Current P&A practices for offshore wells in the North Sea including a description of the used materials and with special emphasize on long-term integrity and cost-efficiency are summarized by Vrålstad et al. (2019). A review of onshore P&A of wells in Canada is given by Trudel et al. (2019).

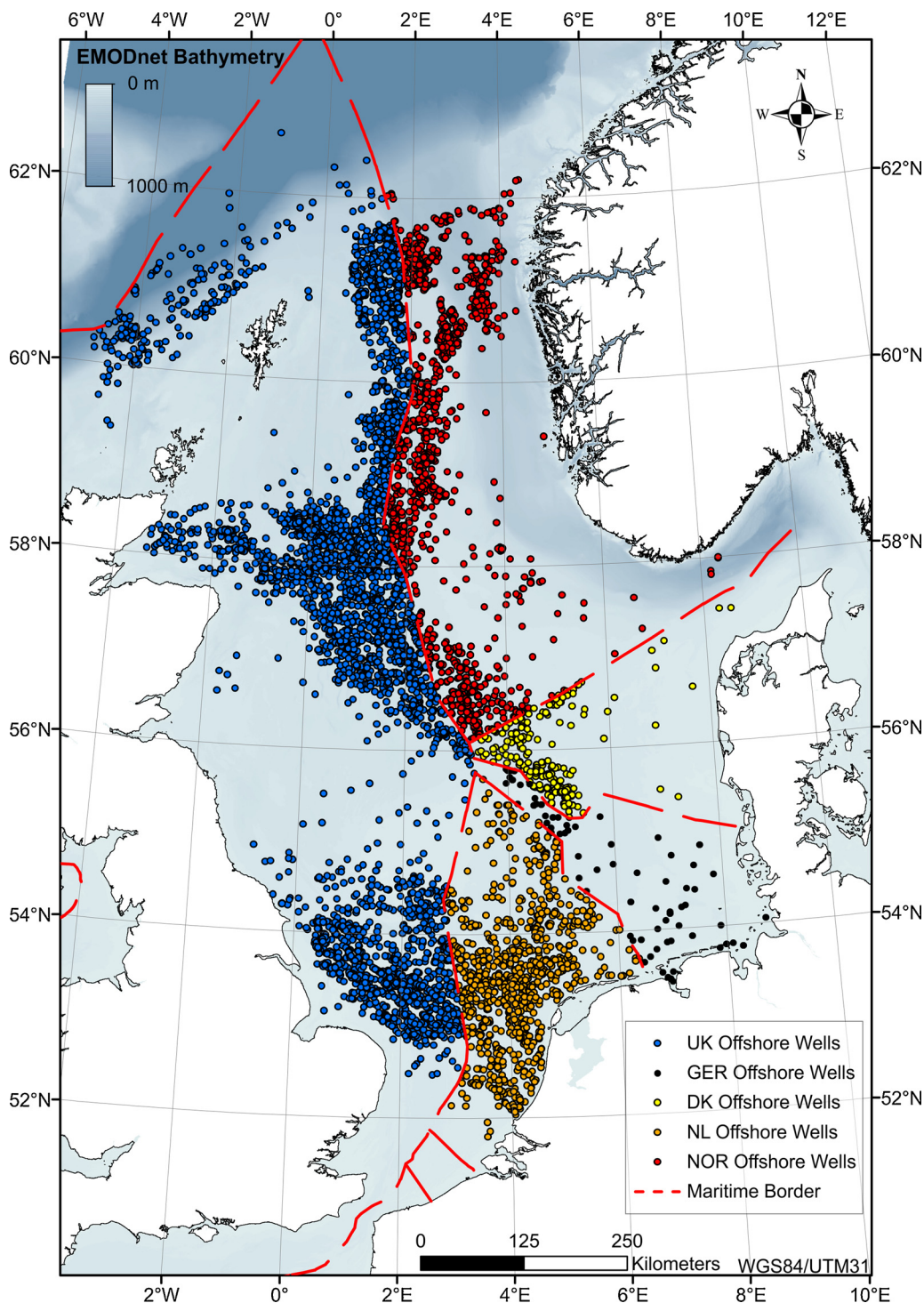The U.K. defines three phases of well P&A operations. In phase 1

Fig. 1. The North Sea comprises of 20,507 documented offshore wells (draped on EMODnet bathymetric data). The wells concentrate in areas where prolific hydrocarbon provinces exist in the subsurface. The well data set comprises of 11,672 UK (UK, blue dots), 6,254 Norwegian (NOR, red dots), 269 Danish (DK, yellow dots), 204 German (GER, black dots) and 2,108 Dutch (NL, orange) offshore wells in the North Sea separated by the maritime border (red dashed line). The available information with respect to these offshore wells is highly variable, however, for all of them at least geographic information, well intent, drilling date and drilling depth exist. See sources for North Sea well inventory in supplement tables S1 & S2.

(AB1) the reservoir is permanently isolated with permanent barrier material. At this stage the tubing may be left in place or is partly or fully retrieved. During Phase 2 (AB2) all intermediate zones with flow potential are permanently isolated with cement or permanent barriers and tubing as well as casing have to be retrieved or milled. The phase is completed when no further permanent barriers are required. In phase 3 (AB3) the wellhead and conductor are removed and if deemed necessary environmental plugs are put in place. Subsequently, the well is considered fully decommissioned never to be used or re-entered again.

Although the principles are the same for onshore and offshore P&A of wells, it is far costlier to abandon wells offshore as they are less accessible and require drilling rigs or intervention vessels (Vrålstad et al., 2019). Decommissioning (incl. all offshore installations) in the U.K. was expected to cost several hundred billion British pounds (GBP), and although recent developments in plugging material and well barrier establishment (e.g. PWC- Perforate, Wash and Cement) have reduced the expected costs significantly, the overall estimated cost for decommissioning all wells in the U.K. offshore areas is still likely to cost about 60 billion GBP (Abshire et al., 2012; UKCS Decommissioning Cost Report, 2017). The largest proportion (45%) of decommissioning costs in the U.K. offshore areas will be run up in the Central North Sea with the largest single item being well abandonment, which amounts to 48% of the total costs and adds up to 28.8 billion GBP (UKCS Decommissioning Cost Report, 2017).

Plugging practices across the North Sea depend on national regulations (Fig. 1). Regulations differ between the countries and concern mainly the plug testing method (weight or pressure tests) and the required length of permanent barriers at the level of the deepest casing shoe (NOR: NORSOK D-010, 2013; DK: Guide to Hydrocarbon Licences in Denmark, 2009; UK: Well Decommissioning Guidelines, 2018; GER: BVOT, 1981; LEBG, 1998; BVEG, 2017; NL: Mining Regulations of the Netherlands, 2014). For instance, U.K. regulations require operators to install a plug length of ~ 30 m (100 feet; Well Decommissioning Guidelines, 2018) while Norwegian regulations require 100 m (50 m if a mechanical plug is used as foundation; NORSOK D-010, 2013; Vrålstad et al., 2019). Today, some regulators require operators to remove all well casing and to cement the sections continuously along the entire borehole, which is referred to as rock-to-rock method (Abshire et al., 2012). While the precise regulations depend on the operator and national/international jurisdiction, these plugs are generally tested in a pressure test to ensure their functionality.

Norway, Denmark, Germany and The Netherlands require at least 100 m-long cement plugs with 50 m above and below potential reservoirs, sources of inflow, or leakage points (NOR: NORSOK D-010, 2013; DK: Guide to Hydrocarbon Licences in Denmark, 2009; GER: BVOT, 1981; LEBG, 1998; NL: Mining Regulations of the Netherlands, 2014). In Germany, the regulations require testing the well barrier integrity via pressure-, weight- or flow tests within three months of plugging and abandonment. In Norway, NORSOK-D010 regulations require pressure tests of the barriers. The regulations in The Netherlands and Denmark do not specify testing methods, but Denmark requires daily reports on performed plugging operations including testing results (DK: Guide to Hydrocarbon Licences in Denmark, 2009; NL: Mining Regulations of the Netherlands, 2014).

None of the above stated regulations in any country require monitoring of the well after plugging and permanent abandonment. While Norwegian regulations recommend excluding zones for drilling activities around shallow gas accumulations, in the UK shallow gas accumulations are considered to occur everywhere and do not necessarily indicate permanent barrier failure (Well Decommissioning Guidelines, 2018). In Norway the costs for well abandonment are significantly higher to meet the self-imposed standards of the operators and official regulations. Furthermore, Norway is the only country that requires monitoring of temporarily suspended wells in form of fluid level and pressure measurements above the shallowest plug when access to the well exists (NORSOK D-010, 2013).

3. Methods

3.1. 3D seismic imaging

We used an extensive industry 3-D seismic dataset ("PGS MegaSurveyPlus") that is a merger of a large number of individual 3-D seismic surveys and covers more than 22,000 km² of the central and northern North Sea from the seafloor down to 1.5 s two-way traveltime (TWT, Figs. 2 and 3). The 3-D dataset was pre-stack time-migrated and the seismic amplitude data (full offset) extend approximately 200 km from north to south and 140 km from east to west. The vertical resolution is approximately 20 m with a spatial resolution of approximately 12.5 m. The data quality varies between the individual datasets depending on acquisition and processing. However, such conventional 3-D reflection seismic datasets have been shown to be useful to identify fluid flow systems, including their geometry, permeability barriers and fluid accumulations, as they manifest themselves in seismic data as amplitude anomalies (Cartwright, 2007).

The investigated 3D seismic data cover 1,792 of a total of 8,969 non-sidetracked wells in the UK sector of the North Sea (i.e. 300 appraisal, 980 development, and 514 exploration wells). We excluded 3,071 sidetracked and multilateral wells from our analysis because of limited information about their exact well paths and because no

sidetracks exist in the upper 1,000 m below the seafloor. Gas release from abandoned wells likely depends on the occurrence of shallow gas in the sedimentary succession. Shallow gas is a generic term to describe gas accumulations in the upper 1000 m below the sea floor and can be identified using direct hydrocarbon indicators, e.g. amplitude anomalies such as bright spots with polarity reversals. We mapped these amplitude anomalies for interpreted seismic horizons with root-mean-square (RMS) amplitude maps.

3.2. Water column imaging

During the cruise POS518 in October 2017, we acquired bathymetric and water column imaging data with the ELAC SEABEAM3050 MKII system, which is designed for very high-resolution imaging of the water column and is mounted to the hull of R/V Poseidon. The system has a 1.5° x 2° transducer, works at a frequency of 50 kHz, and has 191 equi-angle or 386 equi-distant beams. In addition, we used the Imagenex 837B Delta T multibeam for shallow water (260 kHz) to widen the range of frequencies and acquire very high-resolution images of the upper 100 m of the water column. It has a transducer beam width of 120° x 3° and uses 120 beams.

For water column imaging, we used the ELAC WCI Viewer (version 3.21) to process and display data. Water column imaging uses the scattered energy of acoustic signals in the water column and calculates the backscatter intensity (Schneider von Deimling et al., 2007). The system is highly sensitive to any changes in the temperature and density of the water column. We used this system to identify ascending gas bubbles (flares), which originate at the seafloor and align vertically in the water column indicating leakage (Schneider von Deimling et al., 2007). The surveys were planned as intersecting sail lines above known locations of decommissioned hydrocarbon wells to provide high-resolution images of the water column and identify potential gas flares. The water column sound velocity profiles for multibeam processing were measured at the start of every sub-survey using a CTD (conductivity, temperature, depth/pressure) sensor.

Additional water column imaging data were acquired with a newly designed KM SIMRAD ADCP/Echosounder combination (Schmidt et al., 2019), mounted in the moon-pool of R/V Poseidon during cruise POS534 in May 2019. The build-in single-beam echosounder (ES70-18) operates at 70 kHz with a beam angle of 18°. SIMRAD EK80 software controls both, the echosounder and the 170 kHz ADCP and images the water column in high-resolution. The system enables the detection of gas bubbles released at the seafloor, which are visible as a high backscatter anomaly also known as "flares". The lateral drift of the gas bubble plumes can be correlated with simultaneously measured acoustic Doppler current profiles of the water column.

4. Results

4.1. Distribution of shallow gas at different stratigraphic levels in the study area with respect to well location

A ~ 70 km-long seismic profile across the Central Graben of the Central North Sea shows the sedimentary succession down to 1.2 s two-way travel time (TWT) (Fig. 2). Numerous high amplitude anomalies (bright spots) with polarity reversals are present at ~ 5-15 km distance along the profile and at ~ 0.7-0.8 s TWT. These bright spots likely indicate the presence of shallow free gas at about 700 m below the sea level (0.8 s TWT correspond to 640 m at 1,600 m/s seismic velocity). The corresponding seismic horizon can be traced throughout the entire seismic data set and forms a NE-SW oriented trough (Fig. 2). Seismo-stratigraphic correlation of the seismic horizon with literature and well information ties this reflector to the Early Pleistocene (EP, Fig. 2) (Ottesen et al., 2014; Rose et al., 2016). This seismic horizon is characterized by a regional unconformity, which manifests as a zone of chaotic, incoherent reflectors with a corrugated surface and is dissected
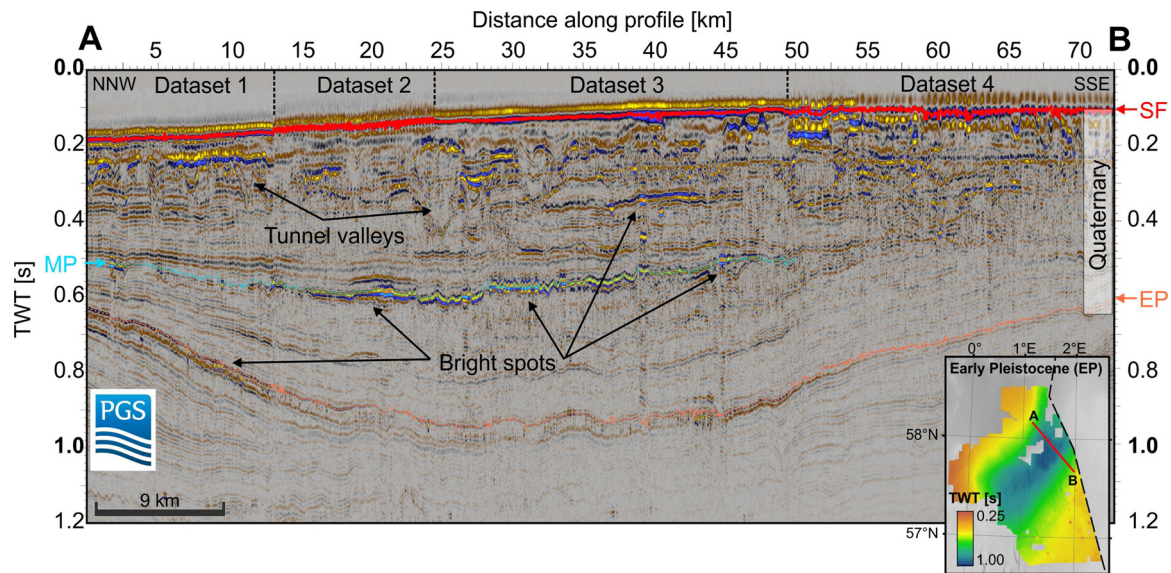
Fig. 2. ~70-km long seismic profile across the Central Graben in the Central North Sea showing the sedimentary succession down to 1.2 s two-way traveltime (TWT). Beneath the seafloor (SF, the Mid-Pleistocene Basin Sands (MP, turquoise line) and the Early Pleistocene Crenulate Marker (EP) are visible as high amplitude anomalies within the Quaternary sedimentary succession (white box indicates the extent of the Quaternary succession). The profile shows distance along the profile in kilometers [km] on the x-axis and the vertical penetration of the seismic energy in seconds [s] of two-way traveltime (TWT) on the y-axis. The location of the profile is shown in the inset. **(INSET)** Map of the seismic Early Pleistocene Crenulate Marker horizon outlining the 3D seismic data set. The red line indicates the location of the seismic profile. The depth of the horizon is given in seconds [s] two-way traveltime (TWT). The map is projected in UTM31/WGS84.

by a large number of linear erosional features. The second prominent horizon is located between 0-50 km distance along profile and at ~ 0.5 s TWT. The seismic horizon shows prominent bright spots with polarity reversals at ~0.55 s TWT and at 2.5 km, between 15-40 km and 45 km distance along profile (Fig. 2). Seismo-stratigraphic correlation ties this reflector to the Mid Pleistocene (MP) (Ottesen et al., 2014; Rose et al., 2016; Reinardy et al., 2017). The seismic facies of the MP horizon is characterized by zones of chaotic, incoherent reflectors with a corrugated surface and is dissected by a large number of tunnel valleys, indicating a regional unconformity (Fig. 2). From the MP horizon upwards to the seafloor (~0.1-0.5 s TWT) numerous bright spots in the sedimentary succession indicate the upward migration of free gas (e.g. at 40 km distance along profile and ~0.3 s TWT). The shallow sedimentary succession is dissected by a large number of tunnel valleys. The seafloor horizon (SF) is a good measure of the data quality. The displayed seismic profile consists of four different 3D seismic data sets (0-13 km, 13-25 km, 25-49 km and 49-72.5 km) with different data qualities shown in this seismic section.

Fig. 3 shows the derived seismic horizons (time structure maps) and RMS amplitude calculations (RMS amplitude maps) and the location of the 3D seismic data set in the North Sea (see Fig. 3a). Imaging of the seafloor morphology is highly dependent on the quality of the seismic data and the applied processing (Fig. 3b). Nevertheless, the seafloor time structure map shows the smooth morphology of the North Sea and water depth ranging between 0.1 and 0.2 s TWT. The EP horizon was traced semi-automated by a combination of manual picks and the IHS Kingdom 3D Seeker + tool across the 3D seismic data set and follows the depression formed by the Central Graben over most of the data and some elevated areas, where the strata is bent upwards (Fig. 3c). Fig. 3d shows RMS amplitudes calculated for the interval between the seafloor plus 50 ms to avoid processing-induced artifacts of the seafloor (SF) reflection and the Early Pleistocene horizon (EP) plus 50 ms. In this way we were able to map all amplitude anomalies (bright spots) within the Quaternary succession, which indicate either a change in lithology or pore space filling, i.e. accumulations of free gas in the upper 1,000 m (shallow gas) (Fig. 2, Fig. 3). There are two prominent provinces, where bright spots occur (Fig. 3d). The first is the central Graben, which dominates the central to northern parts of the seismic data. Here, bright spots are predominantly associated to the two prominent seismic horizons tied to EP and MP (Fig. 2, Fig. 3). The second is the southern part of the survey area, where bright spots are primarily associated with upward-bent sedimentary strata indicating the doming of salt layers from beneath. Above these salt domes, steep-dipping faults dissect the sedimentary succession. Numerous bright spots accompany these geological features at different depth/stratigraphic levels (Fig. 3c-d).

We investigated if gas can be released from the seafloor along any type of well (appraisal, development, exploration) and independently of its status (decommissioned, active). We assumed that shallow gas would have to be present in the vicinity of the well (up to 1 km distance), and an increased permeability induced by the drilling operation and a driving force for gas movement (buoyancy or excess pore pressure). Consequently, we correlated the well paths of 1,792 wells located within the 3D seismic data set with bright spots with polarity reversals indicating shallow gas pockets in the subsurface (Fig. 3b, d). We manually measured that 1,223 of the 1,792 wells are located in close proximity (up to 1 km) to bright spots and thus are potentially sites for gas release from the seafloor.

The quality differences of the individual 3D seismic data sets included in the PGS "MegaSurveyPlus" compilation are clearly visible. Some areas show very high amplitude response in comparison to others and complicate the analysis (see highlighted area in Fig. 3d).

4.2. Mapping of submarine gas flares

We collected water column imaging data along intersecting profiles above selected wells with high seismic RMS amplitude values in close proximity (Fig. 3d). The survey design was chosen to avoid misinterpretation of shoals of fish as flares. We randomly picked 20 wells for detailed surveying of the water column during POS518 using the ELAC SB3050 MKII system (Fig. 4, Fig. 5) and 23 wells during POS534 using a SIMRAD EK80 system (Fig. 5). We note that this way of picking the wells in close proximity to bright spots or high seismic RMS amplitude values, could create a biased data set, but only if wells turn out to leak even further away than the sampled ones. See all results from the water column imaging in our supplementary material (see table S3). Fig. 4 shows three examples of flares identified during cruise POS518,
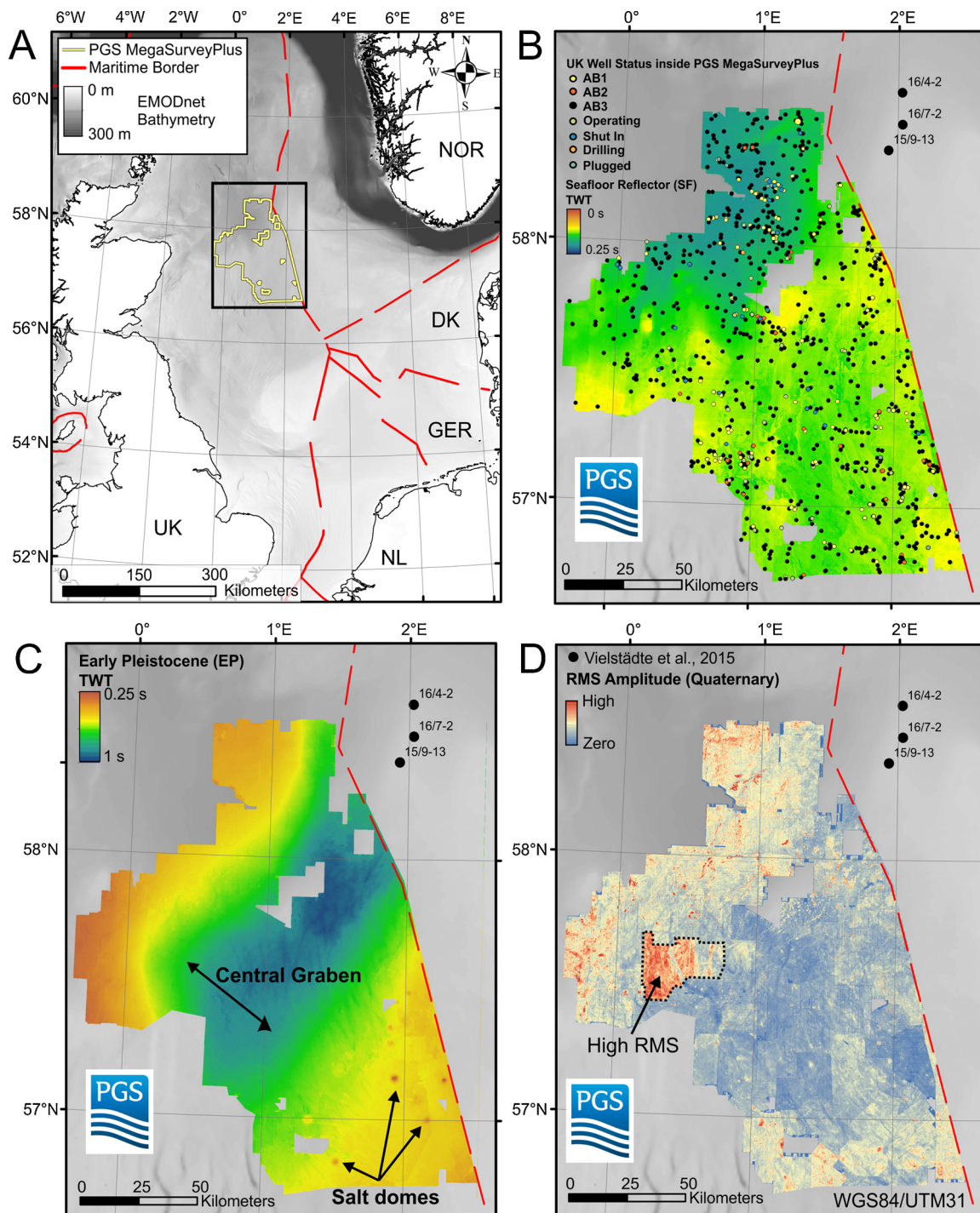
Fig. 3. (A) EMODnet bathymetric map of the North Sea indicating the extent of the 3D seismic data set (yellow line) and the maritime border (dashed red line) separating the UK, Norwegian, Danish, German and Dutch Exclusive Economic Zones (EEZs). The black box indicates the extent of maps B, C, and D. (B) Seismic seafloor horizon showing the location and current status of wells within the 3D seismic data set. AB1-3 = Abandonment phases 1, 2, and 3. (C) Map of the seismic Early Pleistocene (EP) horizon in the 3D seismic data set showing the Central Graben and salt domes in the southern part. Depth is given in seconds [s] TWT. (C) RMS amplitude map of the Quaternary succession showing the spatial distribution of bright spots identified in the 3D seismic data set. Red colors indicate areas with high-amplitude anomalies whereas blue colors indicate low amplitudes. The RMS amplitude is calculated over the time-window from 50 ms beneath the seafloor to 50 ms beneath the EP horizon as indicated in Fig. 2a for the Quaternary succession. Black dots indicate the wells analyzed by Vielstädte et al. (2015). The dashed line indicates an area where the seismic subset shows high RMS amplitude values due to different acquisition and processing procedures resulting in different data quality. In maps B, C, and D the red dashed line indicates the maritime border separating the UK and the Norwegian EEZs.

which are associated with gas release from the seafloor. Fig. 4a displays the fan views of the backscatter intensity in the water column above wells 16/26-3, 16/27a-6 and 16/27b-5. All three fan views show bright anomalies above the wells indicating gas release at the respective seafloor locations (Fig. 4a). Fig. 4b displays fan views that are stacked

along the part of the survey profile close to the well to image the entire flare. This shows that the flares emerge from the seafloor above the well locations and ascend into the water column but that the gas bubbles do not reach the sea surface (Fig. 4).

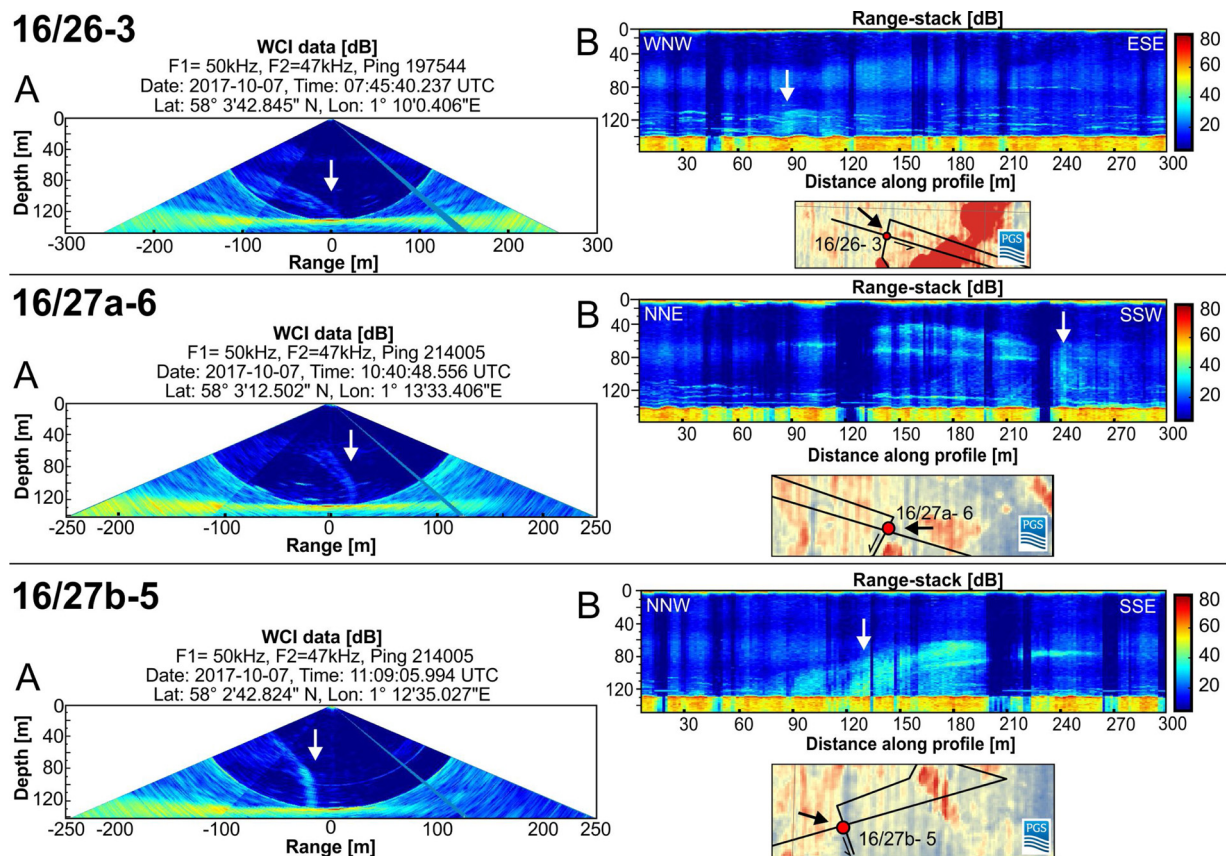Fig. 5 shows the survey lines and the investigated wells draped on

Fig. 4. Water column images acquired with the ELAC SB3050 MKII during POS518 at three decommissioned hydrocarbon well locations (well IDs 16/26-3, 16/27a-6, and 16/27b-5). (A) Fan view at the well locations and (B) the range-stack view along the sailed survey lines as seen in the RMS amplitude maps below (for details see Fig. 5). White arrows indicate the location of the respective wells. Flares at the well locations indicate the leakage of gas from the well head location. The stacked view shows the behavior of the ascending gas bubbles in the water column, which are diverted laterally due to marine currents.

top of the 3D seismic data RMS amplitude map. Red dots indicate wells, where we observed gas flares in the water column while white dots indicate those where no anomalies were found in the water column. In total, we observed gas flares at 28 of the investigated 43 well locations during the two cruises (POS518: 15 of 20 wells, POS534: 13 of 23 wells, see supplementary table S3). 3D seismic data is available for 41 of the investigated 43 wells (Fig. 5). Distances to bright spots with polarity reversals, indicating free gas in the subsurface, vary between 0 and 3300 m.

4.3. Seismic sensitivity analyses for free gas identification

A high amplitude response of the subsurface in the form of bright spots alone is not a direct hydrocarbon indicator (DHI). Bright spots can also be caused by a change in acoustic impedance due to a change in lithology. In the low frequency 3D seismic data used in this study bright spots associated with shallow gas in the subsurface should exhibit reversed polarity in comparison to the seafloor, i.e. a phase shift of 180° (Fig. 6b). Fig. 6a shows a 5-km long seismic section across a typical bright spot in the subsurface located at 0.5 s TWT and lateral extent of ~ 3000 m. This bright spot is associated with the Mid-Pleistocene strata and is in close proximity to wells 16/26-3 and 16/26-24 (see Fig. 6c). The RMS amplitude map indicates one single large bright spot and several smaller bright spots in the surrounding (red color) that suggest possible accumulations of free gas in the Quaternary sediments (see Fig. 6c). To validate that this bright spots is caused by free gas in the subsurface, we calculated the apparent polarity attribute (Fig. 6b), indicating the phase of the reflections seen on the vertical seismic display, for the same area as the RMS amplitude map (Fig. 6c). Bright pink colors indicate areas with polarity reversals and thereby validate that

the formerly identified bright spots are indeed caused by accumulations of free gas in the subsurface.

4.4. Statistical leakage propensity analyses based on well parameters

Well activity data is available for all 43 investigated wells, including e.g. geographic location, spud date (age), deviation type, well intent, abandonment status, drilling depth, water depth. The 43 wells comprise 33 exploration wells, 9 appraisal wells, and 1 development well. All 43 wells are in abandonment phase 3 (AB3), which means that these wells are plugged and abandoned permanently. We measured the distance between all wells of the test group (n = 43) and all those who are within the seismic data set (n = 1,792) and their closest bright spot with polarity reversal. All wells of the test group with a distance to the next bright spot of less than 300 m showed flares in the water column above the well location, indicating gas release from the well (Fig. 5, Fig. 7). Wells that are further away than 1 km from such bright spots with polarity reversals showed no leakage (Fig. 5, Fig. 7).

Furthermore, we calculated the mean RMS amplitudes and RMS amplitude standard deviation for a buffer radius of 300 m around the well paths for all wells inside the seismic data set and the visited wells as 300 m is the distance below which all of the visited wells of the test group showed gas release in form of flares from the seafloor (Fig. 7). Yet Fig. 7 shows that there is no apparent and statistically significant relationship between the propensity to leak and the RMS amplitude and RMS standard deviation. The distribution of spud dates (start of drilling) shows that older wells from the 1970s show higher leakage propensity with a decreasing trend towards wells drilled during the most recent decade (2010-2019) where no leakage is observed (Fig. 7; Supplementary table S3). However, there are only two measurements
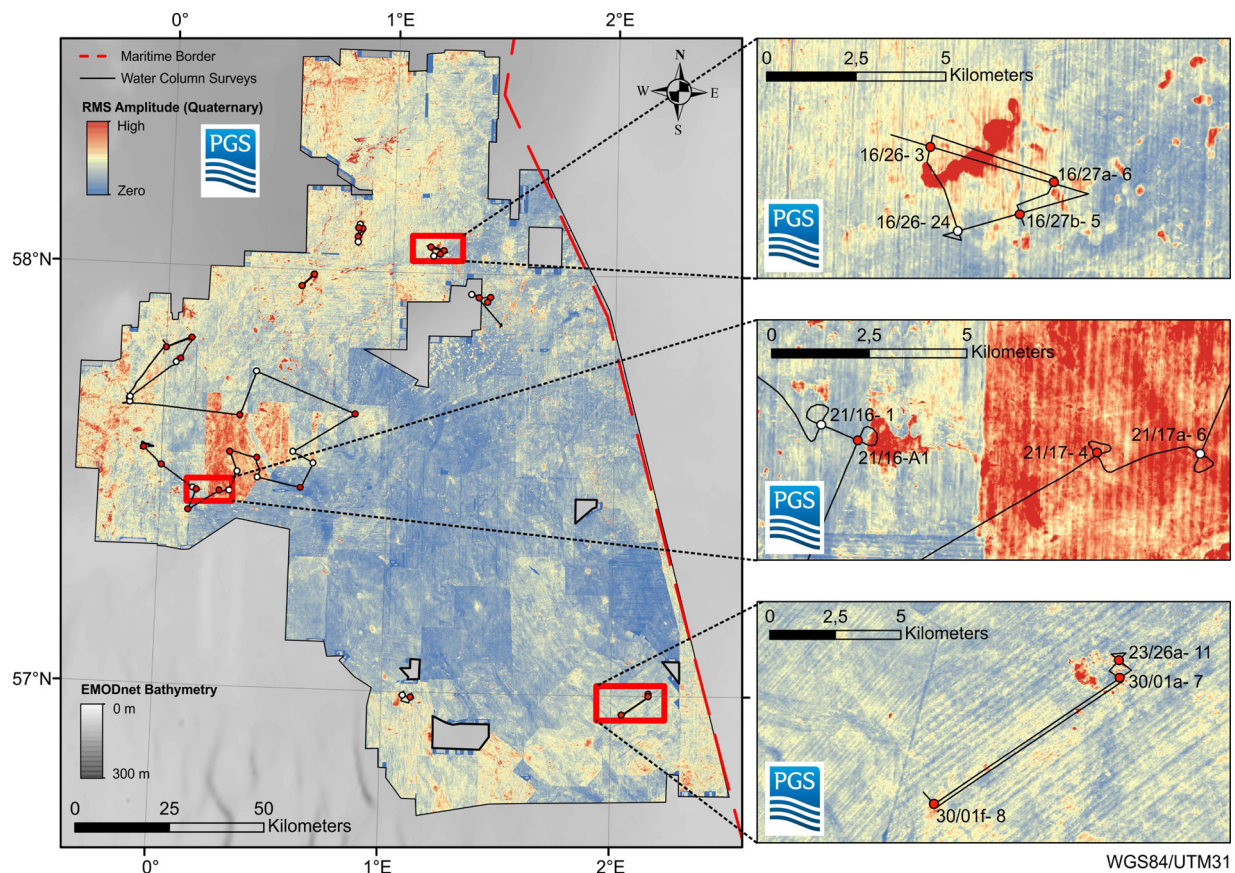
Fig. 5. RMS amplitude map showing the water column imaging surveys (black lines) during POS518 and well leakage identification through flare detection (flares = red dots, no flares = white dots). The red dashed line indicates the maritime border (red dashed line) between the UK and Norway in the Central North Sea. The black dots indicate the locations of wells in the Norwegian sector analyzed by Vielstädte et al. (2015). Further information on well investigation see supplementary material S3.

available from this study for the most recent decade (Fig. 7).

5. Discussion

5.1. Correlation of subsurface gas accumulations and gas flares in the water column

Potential leakage from the investigated decommissioned hydrocarbon wells primarily depends on the occurrence of gas accumulations in the upper 1000 m of the sedimentary succession penetrated by the wells, but also on the local geology, hydraulic connectivity, and rock type (Vielstädte et al., 2015). The analysis of seismic and water column imaging data presented in this study further refines our previous findings by correlating the gas release from abandoned wells with the distance from gas accumulations in the shallow subsurface: Wells that are in close proximity, i.e. within less than 300 m, to bright spots with polarity reversals are likely to leak, whereas wells drilled more than 1000 m away from such shallow gas accumulations do not tend to leak (Fig. 7). For a proper assessment of a well's propensity to leak, however, it is important to further analyze the distribution of gas in the upper 1000 m of the seabed.

5.2. Sources and character of shallow gas in the Central North Sea

The accumulation and migration of free gas and subsequently leakage along the well path is favored in the shallow Quaternary sediments in less than 1000 m below the seafloor as, here, the necessary conditions, i.e. overpressure and local rock strength and tensile strength of unconsolidated sediments are matched (Clayton & Hay, 1994).

Potential gas sources include both upward migrated thermogenic gas from mature source rocks and biogenic gas from geologically young, organic-rich sediments (Judd et al., 1997). Shallow gas in the Central North Sea is primarily associated with two prominent, laterally extensive horizons within the Early to Mid-Pleistocene sediments of the Quaternary succession (Fig. 2). These horizons are known as (1) the Crenulate Marker horizon (Top Unit Z, Ottesen et al., 2014; Rose et al., 2016) and (2) Mid Pleistocene sands (URU-equivalent in Ottesen et al., 2014; R4 in Reinardy et al., 2017). The accumulation of shallow gas, however, is not limited to the Central North Sea. Similar shallow gas accumulations of biogenic origin are documented for many areas across the North Sea, e.g. within the Dutch sector (Schroot & Schüttenhelm, 2003; Kuhlmann & Wong, 2008; Römer et al., 2017), the German sector (Müller et al., 2018), and the Norwegian sector (Vielstädte et al., 2015; Crémière et al., 2016).

The Crenulate Marker is an Early Pleistocene horizon close to the base of the Quaternary and upper Pleistocene sediments, i.e. the base of the Aberdeen Ground Formation. These sediments have been deposited under subglacial, glaciomarine to marine conditions (Sejrup et al., 1987; Stoker & Bent, 1987; Buckley, 2012, 2016; Rose et al., 2016; Reinardy et al., 2017; Rea et al., 2018). The Crenulate Marker is found across the Central North Sea Basin and forms a NE-SW oriented trough (Central Graben) representing a permeable layer, with hydraulic barriers due to deformation by overriding of ice (Rose et al., 2016). At this seismic horizon, shallow gas manifests as bright spots with polarity reversals that are caused by water-bearing reservoirs with free gas saturations of 0-10% (Rose et al., 2016). The Mid Pleistocene basin sands underlie a regional glacial unconformity, which manifests itself in the seismic data by a zone of chaotic, incoherent reflectors with a
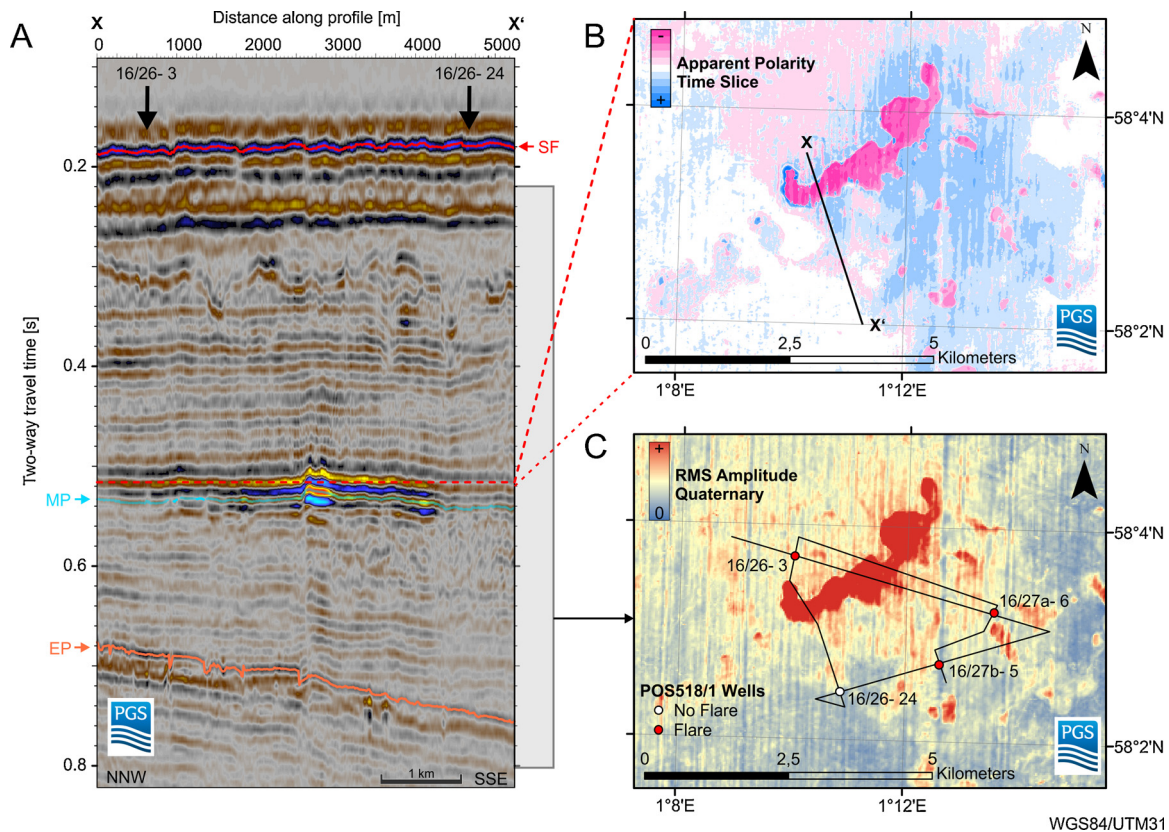
Fig. 6. Sensitivity analysis of the 3D seismic data for bright spots indicating free gas accumulations in the subsurface. Bright spots with polarity reversals indicate gas accumulations whereas other bright spots are predominantly associated to changes in lithology. Exemplarily we show (A) a seismic profile of the 3D seismic data across wells 16/26-3 and 16/26-24 showing the seafloor (SF), Mid-Pleistocene Basin Sands (MP) and the Early Pleistocene Crenulate Marker (EP). (B) 3D seismic attribute analysis using apparent polarity to identify areas with polarity reversal (pink areas). The black line indicates the location of the seismic profile shown in (A). (C) RMS amplitude map of the Quaternary succession showing in red colors bright spots in the subsurface. The black line indicates the sailed survey lines for water column imaging. The RMS amplitude map shows hydrocarbon wells investigated during POS518 showing gas leakage (red dots) and no gas leakage (white dot).

corrugated surface and is dissected by a large number of tunnel valleys. In the center of the Central Graben, numerous bright spots with polarity reversals accompany this unconformity, which are most likely caused by sand bodies deposited during the advance of grounded ice into the North Sea Basin dating to the Mid Pleistocene Transition (~ 1.2-0.5 Ma BP, Reinardy et al., 2017). These sand bodies show increased gas saturations of up to 65% in some areas, e.g. the Aviat Member directly above the Crenulate Member in the central North Sea Basin (Rose et al., 2016). There, the gas in composed mostly of methane (99.9% CH_4) that is isotopically light (average δ^{13}-CH_4 of -69‰ VPDB and average δD-CH_4 of -195‰ VSMOW) indicating a biogenic origin (metabolic CO_2 reduction pathway typical for marine environments) with no thermogenic admixture (Rose et al., 2016).

In the southern part of the survey area, shallow gas accumulations are primarily associated with salt domes (Fig. 5). The salt domes push the overlying sedimentary strata upward and salt migration leads to salt withdrawal basins in between the salt domes. This creates structural traps (i.e. southern North Sea: Ward et al., 2016). Above the salt domes, normal faults form as a result of the gravitational collapse of the overburden sediments that often represent efficient fluid migration pathways (i.e. Tommeliten, Judd & Hovland, 2009). Within these structural traps, biogenic and thermogenic gas may accumulate and possibly mix. Higher order hydrocarbons may be microbially degraded and thus, complicate identifying their origin (Clayton et al., 1997; Nuzzo et al., 2009; Pape et al., 2010; Haffert et al., 2013).

5.3. Migration through the overburden along wells in the Central North Sea

The release of hydrocarbon gases from offshore wells occurs

through two main processes controlling vertical fluid migration. First, leakage may occur through faulty, damaged or corroded well casings and/or annuli (Celia & Bachu, 2003; Gasda et al., 2004) commonly referred to as "well integrity issues". Such migration pathways may open in the microannulus between casing and annular cement, microannulus between cement plug and casing, cracks or channels in cement plugs, rupture or pits in casing resulting in connection between annular cement and wellbore, cracks or channels in annular cement resulting in connections between formation and casing, or through the microannulus between annular cement and formation (Gasda et al., 2004). Second, fluid migration may occur along the outside of the well through drilling-induced fractures surrounding the well path (Harrison et al., 1954; Gurevich et al., 1993; Aadnøy & Bell, 1998; Kårstad & Aadnøy, 2008; Bohnhoff & Zoback; 2010; Osborn et al., 2011; Vielstädte et al., 2015). If present, these fractures are forming anthropogenic pathways through natural/lithological permeability or well barriers (Gurevich et al., 1993; Gasda et al., 2004; Vielstädte et al., 2015), thus connecting deeper strata hydraulically with the seabed (Aydin, 2000; Cartwright, 2007; Løseth et al., 2011). Again, most information on leakage through the fracture networks on the outside of boreholes is related to blowout scenarios (e.g. Leifer & Judd, 2015; Landrø et al., 2019) and currently little quantitative data exist for this type of leakage.

The amount of drilling-induced fractures varies depending on the surrounding lithology, tectonic stress magnitude and orientation, pressure and temperature (Harrison et al., 1954; Aadnøy & Bell, 1998; Brudy & Zoback, 1999; Schroeder et al., 2008; Kårstad and Aadnøy, 2008). In shallow sediments (less than 2-3 km depth), fractures may form laterally and vertically and hydraulically connect subsurface layers (; Bohnhoff & Zoback; 2010; Kårstad and Aadnøy, 2008; Dugan &
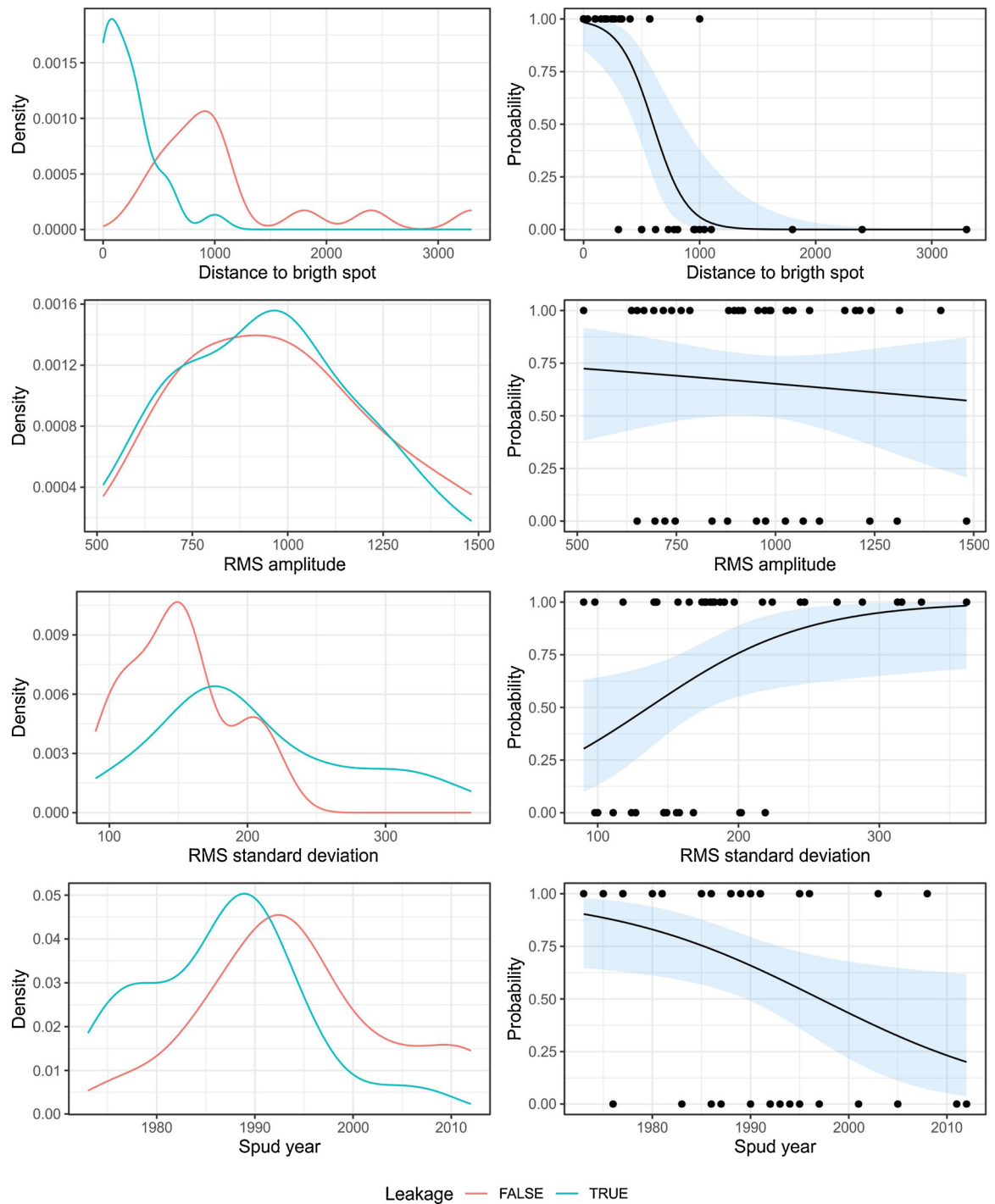
Fig. 7. On the left: Empirical probability density functions (pdf) of the 43 investigated wells, given a leakage (true) or not (false). The pdf is estimated for the variables distance to bright spot with polarity reversal, RMS amplitude, RMS amplitude standard deviation and spud date. On the right: A logistic regression fit for each variable, with a 95% confidence interval based on two standard deviations (i.e. probability of 1 = leakage; 0 = no leakage).

Sheahan, 2012). Such fractures are frequently encountered in cases where the drilling mud is overbalanced (Edwards et al., 2002; Guha et al., 2006). Drilling-induced fractures mechanically weaken the sediment and increase the permeability with regard to the surrounding. The process of focused vertical fluid migration is up to ten times more efficient in areas, where pre-existing natural high-permeability pathways, such as seismic chimneys or pipe structures, exist in the subsurface (Vielstädte et al., 2015). Thus, these drilling-induced fractures may provide fluid migration pathways except for situations in which the mechanical compaction of sediments closes the fractures after drilling

(Bjørlykke & Høeg, 1997; Bjørlykke, 1999). For deeper sections of the boreholes, the induced fractures likely extend less than the diameter of the drill bit outward from the borehole but can reach up to three times the diameter of the drill bit into the surrounding rocks at high pressure and temperature (Brudy & Zoback, 1999). In deeper layers (> 3,000 m), mechanical and chemical compaction may lead to closure of drilling-induced fractures within a short time span, while the upper sedimentary succession may remain hydraulically connected with the seafloor (Bjørlykke & Høeg, 1997).

Geological pre-conditions play a key role in the well's propensity to

leak. Our results show that if the distance between the well and the most proximal bright spot with polarity reversal is shorter than 300 m, leakage is highly likely (100%, 20/20 wells) and for a distance of more than 1,000 m not likely (0/5 wells). For distances in between 300 and 1,000 m, our data show that only 44% (8 of 18) show gas release from the seafloor. Natural seepage from the seafloor in close vicinity to leaking wells (see wells 23/26a-11 & 30/01a-7 in Fig. 5; Linke and Haeckel, 2018) suggests that wells are not necessarily cannibalizing natural release of methane from the seafloor but represent a new, anthropogenic fluid migration pathway. Two geological boundary conditions may explain the increase in leakage probability with decreasing distance. First, lateral gas migration may be favored by dipping beds (up to 1.2-1.4 km distance; Landrø, 2011). Without dipping strata, lateral gas migration for more than 300 m towards the well is unlikely to occur. Second, pre-existing fracture networks may favor the vertical migration of fluids through the overburden (Karstens & Berndt, 2015; Vielstädte et al., 2015). Such fracture networks manifest in seismic data as amplitude anomalies known as seismic chimneys or pipes (Cartwright, 2007; Løseth et al., 2009; Andresen, 2012; Karstens & Berndt, 2015). Measurements at well 16/7-2, which was drilled through such a seismic chimney structure, show ten times higher release rates of up to 19 t of CH_4 per year (Vielstädte et al., 2017). Leakage of shallow gas accumulations along wells thus largely depends on the local lithology and lateral hydraulic connectivity of the subsurface strata. If no pre-existing natural fracture networks or elevated formation permeability exist, the wells connect hydraulically shallow gas accumulations in the subsurface with the seafloor, thereby draining the gas, that otherwise would stay in place over geological times.

5.4. Seismic data limitation and other proxies for leakage from wells

Seismic data can be used to identify areas where gas release from the seafloor is more likely than in other areas. However, their suitability is limited by the quality of the data and homogeneity of the compiled data sets used (see Fig. 2). In our case, areas with systematically elevated (biased) amplitudes limit the quantitative assessment of the well leakage propensity based on RMS amplitudes or RMS amplitude standard deviation. For this reason, we could also not include the seismic data set used in Vielstädte et al. (2015, 2017) as the differences in seismic data processing and data quality are too large.

Bright spots identified in RMS amplitude maps do not necessarily indicate free gas in the subsurface. As we show, it is necessary to identify polarity reversals in combination with the bright spots to ascertain the presence of gas and exclude any false positives. Also, gas mobility depends on its saturation in the pore space (Buckley & Leverett, 1942; Ham & Eilerts, 1967, Gregory, 1976). However, post-stack seismic data alone cannot distinguish between large connected gas bodies and dispersed free gas as all gas occurrences with concentrations above 4 vol. % show as bright spots with reversed polarity (White, 1975; Domenico, 1976; Anstey, 2013). Nevertheless, the correlation between mapped gas and seepage suggests that our approach is permissible, either because some of the gas occurs at high saturation or because also gas at low saturation is mobile enough to reach the wells if the sediment properties are conductive. Subsequent seismic data evaluation can be used to help in estimating methane emission budgets for the central North Sea as it indicates where high probabilities of gas release from the seafloor are to be expected, i.e. where bright spots with polarity reversals are in close proximity of wells.

Other factors, such as the age of wells may also play a role for leakage (Fig. 7; Kang et al., 2016). The age reflects the abandonment techniques and improved drilling and abandonment practices in the past two decades may have decreased the propensity of wells to leak (i.e. Abshire et al., 2012; King & Valencia, 2014). Lateral gas migration towards the well and subsequently along the fractured surrounding of the well is also a matter of time (Landrø et al., 2019) and the lack of evidence for leakage in the water column may simply reflect the fact

that the gas has not yet reached the seafloor. However, our small test group comprises only two wells that are from the last decade (2010-2019) and thus age does not show any statistical relevant trends.

5.5. Leakage propensity prediction based well activity and seismic data in the North Sea

Our analysis indicates that leakage from decommissioned hydrocarbon wells is elevated in areas where seismic amplitude anomalies in the sedimentary succession indicate the presence of shallow gas (Fig. 2, Fig. 4, Fig. 5, Fig. 6, Fig. 7). We test, if the propensity of a well to leak can be identified by using a logistic regression, which includes regressors such as well activity data and/or derived parameters such as mean RMS amplitude and mean RMS amplitude standard deviation, the distance towards the most proximal bright spot with polarity reversal and age (spud date). In order to identify the most suitable regressor combination best subset selection is employed. The main selection criterion chosen was the prediction accuracy from randomly and repeatedly splitting the visited wells into a training and a test set and then using the fitted logistic regression to predict the test data. The most suitable subset turns out to only employ the distance to polarity reversal, producing a prediction accuracy of 89% and the following logistic regression results:

In order to obtain confidence intervals using the normal distribution the distance to bright spot with polarity reversal has to be normally distributed, which it is not. Yet it can be transformed to normality by adding 100 meters to the original distance and then taking the natural logarithm (Table 1).

The transformed logistic regression model is then used to predict the probabilities of leakage for the wells within our seismic data set in the Central North Sea (Fig. 8). In order to obtain confidence bands this logistic regression is performed subtracting and adding two standard deviations from the calculated probability. The point estimate predicts leakage from 926 of the 1,792 wells, where the 95% confidence interval ranges from 719 to 1,058.

Our estimations are derived from only 43 investigated wells, the models which include the regressors distance to bright spot with polarity reversal and spud year or distance, year and well intent reach the same prediction accuracy. Thus, more data on well leakage is needed in order to identify a potentially more precise model. Additional information on well leakage, however, is scarce and little is known about greenhouse gas release associated with decommissioned offshore hydrocarbon wells and in particular in the North Sea. Independent and open access data on greenhouse gas emissions from decommissioned hydrocarbon wells would help to constrain the leakage rates from fossil fuel infrastructure and thus help to derive quantitative conclusions on future well abandonment practices.

5.6. Assessing the rate of methane release

The 20,000 km² of the PGS "Mega Survey Plus" data set comprise 1,792 wells. For our small test group (n = 43) and all wells (n = 1,792) within the boundaries of our seismic data set, we derived the distance towards the most proximal bright spot with polarity reversal and found that for the 1,792 wells an average of 926 wells are likely to leak with a 95% confidence interval ranging from 719 to 1,058 wells (Fig. 8). We

Table 1
Logistic regression fit for leakage of all visited wells using distance to bright spot with polarity reversal in meters as a regressor. Please find further information on the applied statistical analyses in the supplementary material.

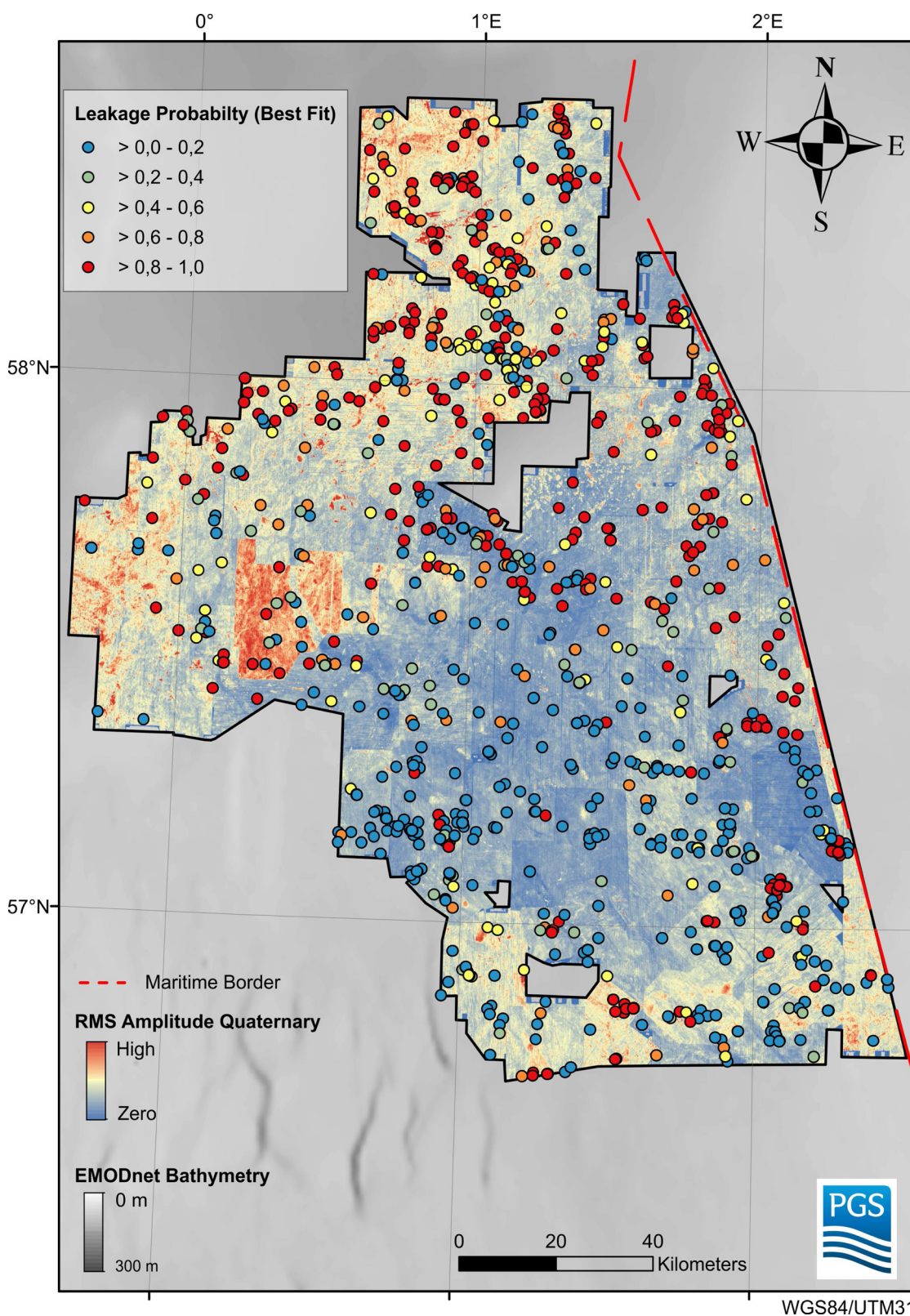|	Estimate	Std. Error	z value	Pr(> |z|)	Significance
Intercept	4,853.946	1,735.128	2.797	0.00515	0.01
Distance	−0.007361	0.002700	−2.726	0.00640	0.01

Fig. 8. The transformed logistic regression model predictions of the probabilities of leakage for the 1,792 wells within the 3-D seismic data set in the Central North Sea. The RMS amplitude map of the 3D seismic data is draped on top of the EMODnet bathymetry map and shows leakage probabilities of the 1,792 wells as color-scaled dots.

combine this approximation of the wells that are likely to leak with the only publicly available gas release rates quantified at marine decommissioned hydrocarbon wells from the Norwegian sector (16/4-2 and 15/9-13; Fig. 3b). Those leaky wells showed biogenic methane release

rates that range between 1 and 4 t of CH$_4$ per year (Vielstädte et al., 2015; most authors are co-authors in this publication). We exclude the high leakage rate of 19 t of CH$_4$ per year determined at well 16/7-2 in the regional emission budget, because this well was drilled in a seismic

Table 2

Compilation of natural and anthropogenic seep sites and their estimates emissions from the seafloor into water column of the North Sea. All values from references are put in relation to the here estimated methane release from marine decommissioned hydrocarbon wells into the water column. Regular font values represent natural seep sites and bold font values represent anthropogenic seep sites. Square brackets give the 95% confidence interval based on two standard deviations.

Site	Leakage Rate [t (CH$_4$) yr^{-1}]	Reference
Block 15/25, UK	6.8	Judd, 2004
Torry Bay, UK	1.2-1.8	Judd et al., 2002
Tommeliten, NO	26	Schneider von Deimling et al., 2011
Anvil Point, UK	68	Hinchcliffe, 1978
Dutch Dogger seep area, NL	478	Römer et al., 2017
Well 16/4-2, NO	**1**	**Vielstädte et al., 2015**
Well 15/9-13, NO	**4**	**Vielstädte et al., 2015**
Well 16/7-2, NO	**19**	**Vielstädte et al., 2015**
CNS Wells, UK	**926-3,704 [719-4,232]**	**This study**
Well 22/4b, UK	**1,751-25,000**	**Leifer, 2015;Sommer et al., 2015**

chimney structure that likely provides a non-representative and highly permeable leakage pathway. We thereby approximate that the average amount of methane that leaks from wells to be 0.9-3.7 [0.7-4.2] kt yr^{-1} of CH$_4$ for 1,792 wells spread over 20,000 km^2 of the UK sector in the Central North Sea (Table 2, Fig. 8). Square brackets give the range of the 95% confidence interval based on two standard deviations, i.e. 1-4 t yr^{-1} of CH$_4$ for 719-1,058 wells. However, more direct measurements of gas release from boreholes through remotely operated vehicles are necessary to further improve the results. Despite the uncertainty of this estimate, it is in good agreement with our previously estimated regional leakage rate of 3-17 kt yr^{-1} of CH$_4$ for a total of 11,122 wells in the North Sea (Vielstädte et al., 2017).

Inadvertent methane emissions from decommissioned hydrocarbon wells are thus a major source of methane into the North Sea (Table 2). We show that the sum of all methane emissions from decommissioned hydrocarbon wells is only exceeded by high-emission blow-out sites (e.g. 22/4b, UK; Leifer; 2015). In comparison to the natural release of greenhouse gas (methane) into the water column of the North Sea, the release of greenhouse gases from marine decommissioned hydrocarbon wells is likely to be a significant source and larger than all known natural seepage sites combined. Shallow gas is not only a local phenomenon to the investigated area but occurs also in other areas of the North Sea (Schroot & Schüttenhelm, 2003; Kuhlmann & Wong, 2008; Crémière et al., 2016; Römer et al., 2017; Müller et al., 2018). Thus, the potential for leakage from marine decommissioned hydrocarbon wells is given where such shallow gas accumulations exist in the subsurface (Vielstädte et al., 2015). An identification of shallow gas in correlation with drilled wells is needed on a regional to global scale to update the estimates of methane emissions from fossil fuels. This is particularly important on land as drilling-induced leakage along wells in this setting emits the methane directly into the atmosphere, because the mitigating water column is absent. Thus, decommissioned wells may play a key role in methane gas emissions from hydrocarbon provinces, particularly on land, and consequently should be monitored.

5.7. Suggestions for improved drilling and abandonment practice

We show that leakage from decommissioned hydrocarbon wells is primarily associated with gas accumulations in the upper 1,000 m of the sedimentary succession. Here, both biogenic and thermogenic gases may rise along vertical, permeable fluid migration pathways such as wells, chimneys and pipes or faults and the associated fractures. We propose that drilling practice should consider shallow gas accumulations not only as a drilling hazard, but also take into consideration their potential for drilling-induced hydrocarbon gas release. Ideally, drilling operations should avoid gas accumulations by a distance of at least one kilometer to minimize the risk of leakage. This distance will depend on the local lithology and permeability of hydraulically conductive layers in the sedimentary record and should be analyzed carefully based on

local/regional geological information prior to starting any drilling operations.

In global perspective, the North Sea has a relatively short history of drilling for hydrocarbons with the first commercial well drilled in 1950 (German well CUXH 1001, see table S1). Plugging and abandonment practices have improved significantly over the past decades and likely retain fluids within their respective reservoir (Trudel et al., 2019; Vrålstad et al. 2019). In contrast, California has a more than 150 year-long record of oil and gas development since the first commercial well in 1865, and old wells tend to be poorly documented and abandoned (Kang et al., 2014, 2016), which likely makes these wells potentially unrecognized emitters of thermogenic gas from the deep reservoir. However, in the North Sea, there have been no indications for hydrocarbon emissions from the deep-seated reservoir so far. Instead, in this and our previous studies (Vielstädte et al., 2015, 2017) we have documented that wells pose a high risk for leakage of biogenic methane from gas accumulations in the upper 1,000 m, if drilled through or in close proximity to those shallow gas pockets. Therefore, monitoring of wells (e.g. through acoustic water column imaging and water/gas sampling in case of leakage identification) should not end after their abandonment. This would not only help to constrain the methane emissions from fossil fuel infrastructure, but also to understand if and how quickly well barriers degrade (in the case of leakage from the deep reservoirs). This should be used to improve plugging and abandonment standards.

6. Conclusions

We document gas release from decommissioned hydrocarbon wells by using water column imaging in combination with 3D seismic data. We show that 28 out of 43 investigated wells show indications for gas release from the seafloor into the water column. We assess their probability to leak based on a logistic regression using the distance to bright spot with polarity reversal. This work flow is a suitable tool to predict leakage of hydrocarbon gases from abandoned wells with a high probability. However, independent and open access data on greenhouse gas emissions from decommissioned hydrocarbon wells would help to constrain the leakage rates from fossil fuel infrastructure.

Gas release from wells in the North Sea largely depends on the presence of shallow gas accumulations (i.e. in the upper 1,000 m below the seabed) and their proximity to the wells (i.e. less than 1,000 m distance). These shallow, biogenic gas accumulations are sourced primarily from geologically young, organic-rich Neogene sediments. Gas from deeper, thermogenic reservoirs may also contribute to the formation of these shallow gas accumulations, e.g. if hydraulic connections to the shallow subsurface exist. Leakage is highly variable depending on the local lithology as well as the lateral hydraulic connection to deeper strata, e.g. dipping beds may deviate the gas flow in the subsurface. As a leakage mitigation measure, wells should be

drilled in sufficient distance from such shallow gas accumulations.

In the upper 1,000 m below the seafloor, gas migration is likely focused along the fractures induced by the drilling procedure around the well path. Below 1,000 m sediment depth, the plugging and abandonment practices and the protective measures stipulated by local regulations and guidelines have improved over the past decades. This likely prevents the ascent of deep reservoir fluids. However, none of the guidelines and protective measures include monitoring of the wells, neither directly after permanent abandonment nor in the long term, but this would help to improve not only the estimates of methane released from decommissioned hydrocarbon wells but it would also help to improve the plugging and abandonment standards. We therefore recommend not only to monitor wells during the initial period after plugging and abandonment, but also to have repeated long-term monitoring surveys of the water column.

Here, we show that small emissions from single hydrocarbon wells in the UK sector of the central North Sea may accumulate to a significant contribution of 0.9-3.7 [95% confidence interval = 0.7-4.2] kt yr^{-1} of CH_4 (from 1,792 wells in an area of 20,000 km^2). Considering that likely similar geologic conditions exist across the North Sea and with respect to the more than 20,507 hydrocarbon wells (currently 6689 decommissioned, not considering the multi-lateral wells drilled in > 1 km sediment depth), the large number of wells likely constitute a major source of methane in the North Sea. However, information on methane emissions from fossil fuel infrastructure almost always originates from the oil and gas industry itself. Independent emission estimates are scarce. In the U.S., for example, studies have shown that the numbers provided by the industry are too low (Allen et al., 2013; Miller et al., 2013). Further independent emission measurements are needed for the development of guidelines and legally binding regulations.

Conflict of interests

The authors declare that they have no known competing financial interests or personal relationships that could have appeared to influence the work reported in this paper.

CRediT authorship contribution statement

Christoph Böttner: Conceptualization, Data curation, Formal analysis, Investigation, Methodology, Visualization, Writing - original draft, Writing - review & editing. **Matthias Haeckel:** Conceptualization, Funding acquisition, Investigation, Project administration, Resources, Supervision, Writing - original draft, Writing - review & editing. **Mark Schmidt:** Conceptualization, Funding acquisition, Investigation, Project administration, Resources, Supervision, Writing - original draft, Writing - review & editing. **Christian Berndt:** Conceptualization, Funding acquisition, Project administration, Resources, Supervision, Writing - original draft, Writing - review & editing. **Lisa Vielstädte:** Conceptualization, Investigation, Writing - original draft. **Jakob A. Kutsch:** Methodology, Resources, Formal analysis, Software, Visualization, Writing - review & editing. **Jens Karstens:** Investigation, Supervision, Writing - original draft. **Tim Weiß:** Data curation, Investigation, Resources, Software, Writing - original draft.

Declaration of Competing Interest

The authors report no declarations of interest.

Appendix A. Supplementary data

Supplementary material related to this article can be found, in the online version, at doi:https://doi.org/10.1016/j.ijggc.2020.103119.

References

Aadnøy, B.S., Bell, J.S., 1998. Classification of drilling-induced fractures and their relationship to in-situ stress directions. The Log Analyst 39 (06).

Abshire, L.W., Desai, P., Mueller, D., Paulsen, W.B., Robertson, R.D., Solheim, T., 2012. Offshore permanent well abandonment. Oilfield Review 24 (1), 42–50.

Allen, D.T., Torres, V.M., Thomas, J., Sullivan, D.W., Harrison, M., Hendler, A., ... Lamb, B.K., 2013. Measurements of methane emissions at natural gas production sites in the United States. Proceedings of the National Academy of Sciences 110 (44), 17768–17773.

Andresen, K.J., 2012. Fluid flow features in hydrocarbon plumbing systems: What do they tell us about the basin evolution? Marine Geology 332, 89–108.

Anstey, N.A., 2013. Seismic interpretation: the physical aspects. Springer Science & Business Media.

Aydin, A., 2000. Fractures, faults, and hydrocarbon entrapment, migration and flow. Marine and Petroleum Geology 17 (7), 797–814.

Berndt, C., 2005. Focused fluid flow in passive continental margins. Philosophical Transactions of the Royal Society A: Mathematical, Physical and Engineering Sciences 363 (1837), 2855–2871.

Berndt, C., Bünz, S., Mienert, J., 2003. Polygonal fault systems on the mid-Norwegian margin: a long-term source for fluid flow. Geological Society, London, Special Publications 216 (1), 283–290.

Bjørlykke, K., 1999. Principal aspects of compaction and fluid flow in mudstones. Geological Society, London, Special Publications 158 (1), 73–78.

Bjørlykke, K., Høeg, K., 1997. Effects of burial diagenesis on stresses, compaction and fluid flow in sedimentary basins. Marine and Petroleum Geology 14 (3), 267–276.

Bohnhoff, M., Zoback, M.D., 2010. Oscillation of fluid-filled cracks triggered by degassing of CO2 due to leakage along wellbores. Journal of Geophysical Research: Solid Earth 115 (B11).

Böttner, C., Berndt, C., Reinardy, B.T., Geersen, J., Karstens, J., Bull, J.M., ... Schramm, B., 2019. Pockmarks in the Witch Ground Basin, Central North Sea. Geochemistry, Geophysics, Geosystems 20 (4), 1698–1719.

Brandt, A.R., Heath, G.A., Kort, E.A., O'sullivan, F., Pétron, G., Jordaan, S.M., ... Wofsy, S., 2014. Methane leaks from North American natural gas systems. Science 343 (6172), 733–735.

Brudy, M., Zoback, M., 1999. Drilling-induced tensile wall-fractures: implications for determination of in-situ stress orientation and magnitude. International Journal of Rock Mechanics and Mining Sciences 36 (2), 191–215.

Buckley, F.A., 2012. An early Pleistocene grounded ice sheet in the Central North Sea. Geological Society, London, Special Publications 368 (SP368–8(1)), 185–209. https://doi.org/10.1144/SP368.8.

Buckley, F.A., 2016. A glaciogenic sequence from the Early Pleistocene of the Central North Sea. Journal of Quaternary Science 32 (2), 145–168.

Buckley, S.E., Leverett, M., 1942. Mechanism of fluid displacement in sands. Transactions of the AIME 146 (01), 107–116.

BVEG, 2017. Bundesverband Erdgas, Erdöl und Geoenergie e.V. Technische Regel Bohrungsintegrität. Bundesverband Erdgas, Erdöl und Geoenergie e.V, Hannover, Deutschland.

BVOT, 1981. Landesverordnung –Bergverordnung über Tiefbohrungen, Tiefspeicher und die Gewinnung von Bodenschätzen durch Bohrungen im Lande Schleswig-Holstein (Tiefbohrverordnung – BVOT), GVOBl. Schl.-H. S. 264. Oberbergamt für das Land Schleswig-Holstein, Clausthal-Zellerfeld, Deutschland.

Cartwright, J., 2007. The impact of 3D seismic data on the understanding of compaction, fluid flow and diagenesis in sedimentary basins. Journal of the Geological Society 164 (5), 881–893. https://doi.org/10.1144/0016-76492006-143.

Celia, M.A., Bachu, S., 2003. Geological sequestration of CO2: is leakage unavoidable and acceptable? Greenhouse Gas Control Technologies-6th International Conference. Pergamon, pp. 477–482 (January).

Ciais, P., Sabine, C., Bala, G., Bopp, L., Brovkin, V., Canadell, J., et al., 2013. Carbon and other biogeochemical cycles. Climate change 2013: The physical science basis. Contribution of Working Group I to the Fifth Assessment Report of the Intergovernmental Panel on Climate Change. Cambridge University Press, United Kingdom and New York, NY, USA, pp. 465–570.

Clayton, C.J., Hay, S.J., 1994. Gas migration mechanisms from accumulation to surface. Bulletin of the Geological Society of Denmark 41 (1), 12–23.

Clayton, C.J., Hay, S.J., Baylis, S.A., Dipper, B., 1997. Alteration of natural gas during leakage from a North Sea salt diapir field. Marine Geology 137 (1-2), 69–80.

Crémière, A., Lepland, A., Chand, S., Sahy, D., Kirsimäe, K., Bau, M., ... Brunstad, H., 2016. Fluid source and methane-related diagenetic processes recorded in cold seep carbonates from the Alvheim channel, central North Sea. Chemical Geology 432, 16–33.

Domenico, S.N., 1976. Effect of brine-gas mixture on velocity in an unconsolidated sand reservoir. Geophysics 41 (5), 882–894.

Dugan, B., Sheahan, T.C., 2012. Offshore sediment overpressures of passive margins: Mechanisms, measurement, and models. Reviews of Geophysics 50 (3).

Dumke, I., Berndt, C., Crutchley, G.J., Krause, S., Liebetrau, V., Gay, A., Couillard, M., 2014. Seal bypass at the Giant Gjallar Vent (Norwegian Sea): Indications for a new phase of fluid venting at a 56-Ma-old fluid migration system. Marine Geology 351, 38–52.

Edwards, S.T., Bratton, T.R., Standifird, W.B., 2002. Accidental Geomechanics-Capturing In-situ Stress from Mud Losses Encountered while Drilling (January). SPE/ISRM rock mechanics conference. Society of Petroleum Engineers.

Gasda, S.E., Bachu, S., Celia, M.A., 2004. Spatial characterization of the location of potentially leaky wells penetrating a deep saline aquifer in a mature sedimentary basin. Environmental Geology 46 (6-7), 707–720.

Gregory, A.R., 1976. Fluid saturation effects on dynamic elastic properties of sedimentary rocks. Geophysics 41 (5), 895–921.

Guha, R., Tyagi, A.K., Corley, B., Rabinovich, M., Tang, X., 2006. Integrating multi-sensor acoustic and resistivity data for improved formation evaluation in the presence of drilling induced fractures (January). SPWLA 47th Annual Logging Symposium. Society of Petrophysicists and Well-Log Analysts.

Guide to Hydrocarbon Licences in Denmark, 2009. General Legislation and Information Exploration and Drilling Activities, Subchapter Guidelines for Drilling. Danish Energy Agency, Copenhagen, Denmark, pp. 228.

Gurevich, A.E., Endres, B.L., Robertson Jr., J.O., Chilingar, G.V., 1993. Gas migration from oil and gas fields and associated hazards. Journal of Petroleum Science and Engineering 9 (3), 223–238.

Haffert, L., Haeckel, M., Liebetrau, V., Berndt, C., Hensen, C., Nuzzo, M., ... Weise, S.M., 2013. Fluid evolution and authigenic mineral paragenesis related to salt diapirism–The Mercator mud volcano in the Gulf of Cadiz. Geochimica et Cosmochimica Acta 106, 261–286.

Ham, J.D., Eilerts, C.K., 1967. Effect of saturation on mobility of low liquid-vapor ratio fluids. Society of Petroleum Engineers Journal 7 (01), 11–19.

Harrison, E., Kieschnick, W.F., McGuire, W.J., 1954. The Mechanics of Fracture Induction and Extension. AIME Petroleum Transactions 201, 252–263.

Hinchcliffe, J.C., 1978. Death stalks the secret coast. Triton 23 (2), 56–57.

Hubbert, M.K., Willis, D.G., 1957. Mechanic of hydraulic fracturing. Trans. Soc. Pet. Eng. AIME 1957, 153–168.

Judd, A.G., Sim, R., Kingston, P., McNally, J., 2002. Gas seepage on an intertidal site: Torry Bay, Firth of Forth. Scotland. Continental Shelf Research 22 (16), 2317–2331.

Judd, A.G., 2004. Natural seabed gas seeps as sources of atmospheric methane. Environmental Geology 46 (8), 988–996.

Judd, A., Hovland, M., 2009. Seabed fluid flow: the impact on geology, biology and the marine environment. Cambridge University Press.

Judd, A., Davies, G., Wilson, J., Holmes, R., Baron, G., Bryden, I., 1997. Contributions to atmospheric methane by natural seepages on the UK continental shelf. Marine Geology 137 (1-2), 165–189.

Kang, M., Christian, S., Celia, M.A., Mauzerall, D.L., Bill, M., Miller, A.R., ... Jackson, R.B., 2016. Identification and characterization of high methane-emitting abandoned oil and gas wells. Proceedings of the National Academy of Sciences 113 (48), 13636–13641.

Kang, M., Kanno, C.M., Reid, M.C., Zhang, X., Mauzerall, D.L., Celia, M.A., ... Onstott, T.C., 2014. Direct measurements of methane emissions from abandoned oil and gas wells in Pennsylvania. Proceedings of the National Academy of Sciences 111 (51), 18173–18177.

Kårstad, E., Aadnøy, B.S., 2008. Improved prediction of shallow sediment fracturing for offshore applications. SPE Drilling & Completion 23 (02), 88–92.

Karstens, J., Berndt, C., 2015. Seismic chimneys in the Southern Viking Graben–Implications for palaeo fluid migration and overpressure evolution. Earth and Planetary Science Letters 412, 88–100.

King, G.E., Valencia, R.L., 2014. Environmental risk and well integrity of plugged and abandoned wells. SPE Annual Technical Conference and Exhibition. Society of Petroleum Engineers, Amsterdam.

Kuhlmann, G., Wong, T.E., 2008. Pliocene paleoenvironment evolution as interpreted from 3D-seismic data in the southern North Sea, Dutch offshore sector. Marine and Petroleum Geology 25 (2), 173–189.

Landrø, M., 2011. Seismic monitoring of an old underground blowout–20 years later. First Break 29 (6), 39–48.

Landrø, M., Wehner, D., Vedvik, N., Ringrose, P., Løhre, N.L., Berteussen, K., 2019. Gas flow through shallow sediments—A case study using passive and active seismic field data. International Journal of Greenhouse Gas Control 87, 121–133.

Le Quéré, C., Andrew, R.M., Friedlingstein, P., Sitch, S., Hauck, J., Pongratz, J., ... Arneth, A., 2018. Global carbon budget 2018. Earth System Science Data (Online) 10 (4).

LEBG, 1998. Richtlinie des Oberbergamtes in Clausthal-Zellerfeld über das Verfüllen auflässiger Bohrungen. Oberbergamt, Clausthal-Zellerfeld, Deutschland.

Leifer, I., 2015. Seabed bubble flux estimation by calibrated video survey for a large blowout seep in the North Sea. Marine and Petroleum Geology 68, 743–752.

Leifer, I., Judd, A., 2015. The UK22/4b blowout 20 years on: Investigations of continuing methane emissions from sub-seabed to the atmosphere in a North Sea context. Marine and Petroleum Geology 68, 706–717.

Linke, P., Haeckel, M., 2018. RV POSEIDON Fahrtbericht/Cruise Report POS518: Baseline Study for the Environmental Monitoring of Subseafloor CO2 Storage Operations, Leg 1: Bremerhaven–Bremerhaven (Germany) 25.09.-11.10. 2017, Leg 2: Bremerhaven–Kiel (Germany) 12.10.-28.10. 2017.

Løseth, H., Gading, M., Wensaas, L., 2009. Hydrocarbon leakage interpreted on seismic data. Marine and Petroleum Geology 26 (7), 1304–1319.

Løseth, H., Wensaas, L., Arntsen, B., Hanken, N.M., Basire, C., Graue, K., 2011. 1000 m long gas blow-out pipes. Marine and Petroleum Geology 28 (5), 1047–1060.

Marfurt, K.J., Alves, T.M., 2015. Pitfalls and limitations in seismic attribute interpretation of tectonic features. Interpretation 3 (1), SB5–SB15.

Miller, S.M., Wofsy, S.C., Michalak, A.M., Kort, E.A., Andrews, A.E., Biraud, S.C., ... Miller, B.R., 2013. Anthropogenic emissions of methane in the United States. Proceedings of the National Academy of Sciences 110 (50), 20018–20022.

Mining Regulations of the Netherlands, 2014. Regulations of the Staatssecretaris of Economic Affairs of 16 December 2002/nr WJZ 02063603 regulating the implementation of the Mijnbouwbesluit (2003, updated). Dorhout Advocaten N.V, Groningen, Netherlands.

Müller, S., Reinhardt, L., Franke, D., Gaedicke, C., Winsemann, J., 2018. Shallow gas accumulations in the German North Sea. Marine and Petroleum Geology 91, 139–151.

Nordbotten, J.M., Celia, M.A., Bachu, S., 2004. Analytical solutions for leakage rates through abandoned wells. Water Resources Research 40 (4).

Nordbotten, J.M., Celia, M.A., Bachu, S., Dahle, H.K., 2005. Semianalytical solution for CO2 leakage through an abandoned well. Environmental Science & Technology 39 (2), 602–611.

NORSOK D-010, 2013. Well integrity in drilling and well operations, NORSOK Standard D-010 (Rev. 4). Standards Norway, Lysaker, Norway.

Nuzzo, M., Hornibrook, E.R., Gill, F., Hensen, C., Pancost, R.D., Haeckel, M., ... Pinheiro, L.M., 2009. Origin of light volatile hydrocarbon gases in mud volcano fluids, Gulf of Cadiz—evidence for multiple sources and transport mechanisms in active sedimentary wedges. Chemical Geology 266 (3-4), 350–363.

Osborn, S.G., Vengosh, A., Warner, N.R., Jackson, R.B., 2011. Methane contamination of drinking water accompanying gas-well drilling and hydraulic fracturing. Proceedings of the National Academy of Sciences 108 (20), 8172–8176.

Ottesen, D., Dowdeswell, J.A., Bugge, T., 2014. Morphology, sedimentary infill and depositional environments of the Early Quaternary North Sea Basin (56–62 N). Marine and Petroleum Geology 56, 123–146.

Pape, T., Bahr, A., Rethemeyer, J., Kessler, J.D., Sahling, H., Hinrichs, K.U., ... Bohrmann, G., 2010. Molecular and isotopic partitioning of low-molecular-weight hydrocarbons during migration and gas hydrate precipitation in deposits of a high-flux seepage site. Chemical Geology 269 (3-4), 350–363.

Rea, B.R., Newton, A.M., Lamb, R.M., Harding, R., Bigg, G.R., Rose, P., et al., 2018. Extensive marine-terminating ice sheets in Europe from 2.5 million years ago. Science Advances 4 (6). https://doi.org/10.1126/sciadv.aar8327. eaar8327.

Reinardy, B.T., Hjelstuen, B.O., Sejrup, H.P., Augedal, H., Jørstad, A., 2017. Late Pliocene-Pleistocene environments and glacial history of the northern North Sea. Quaternary Science Reviews 158, 107–126. https://doi.org/10.1016/j.quascirev.2016.12.022.

Römer, M., Wenau, S., Mau, S., Veloso, M., Greinert, J., Schlüter, M., Bohrmann, G., 2017. Assessing marine gas emission activity and contribution to the atmospheric methane inventory: A multidisciplinary approach from the Dutch Dogger Bank seep area (North Sea). Geochemistry, Geophysics, Geosystems 18 (7), 2617–2633.

Rose, P., Byerley, G., Vaughan, O., Cater, J., Rea, B.R., Spagnolo, M., Archer, S., 2016. Aviat: A Lower Pleistocene shallow gas hazard developed as a fuel gas supply for the Forties Field. Geological Society, London, petroleum geology conference series, (Vol. 8, pp. PGC8–PGC16). Geological Society of London, London.

Saunois, M., Bousquet, P., Poulter, B., Peregon, A., Ciais, P., Canadell, J.G., et al., 2016. The global methane budget 2000–2012. Earth System Science Data 8 (2), 697–751. https://doi.org/10.5194/essd-8-697-2016.

Schmidt, M., et al., 2019. RV POSEIDON Fahrtbericht/Cruise Report POS534: STEMM-CCS Study of the Environmental Monitoring of Subseafloor CO2 Storage Operations. Bremerhaven-Kiel (Germany) 01.05.-29.05.2019.

Schneider von Deimling, J., Brockhoff, J., Greinert, J., 2007. Flare imaging with multibeam systems: Data processing for bubble detection at seeps. Geochemistry, Geophysics, Geosystems 8 (6).

Schneider von Deimling, J., Rehder, G., Greinert, J., McGinnnis, D.F., Boetius, A., Linke, P., 2011. Quantification of seep-related methane gas emissions at Tommeliten. North Sea. Continental Shelf Research 31 (7-8), 867–878.

Schroot, B.M., Schüttenhelm, R.T.E., 2003. Expressions of shallow gas in the Netherlands North Sea. Netherlands Journal of Geosciences 82 (1), 91–105.

Sejrup, H.P., Aarseth, I., Ellingsen, K.L., Reither, E., Jansen, E., Løvlie, R., et al., 1987. Quaternary stratigraphy of the Fladen area, central North Sea: A multidisciplinary study. Journal of Quaternary Science 2 (1), 35–58. https://doi.org/10.1002/jqs.3390020105.

Sommer, S., Schmidt, M., Linke, P., 2015. Continuous inline mapping of a dissolved methane plume at a blowout site in the Central North Sea UK using a membrane inlet mass spectrometer–Water column stratification impedes immediate methane release into the atmosphere. Marine and Petroleum Geology 68, 766–775.

Stoker, M.S., Bent, A.J., 1987. Lower Pleistocene deltaic and marine sediments in boreholes from the central North Sea. Journal of Quaternary Science 2 (2), 87–96. https://doi.org/10.1002/jqs.3390020202.

Townsend-Small, A., Ferrara, T.W., Lyon, D.R., Fries, A.E., Lamb, B.K., 2016. Emissions of coalbed and natural gas methane from abandoned oil and gas wells in the United States. Geophysical Research Letters 43 (5), 2283–2290.

Trudel, E., Bizhani, M., Zare, M., Frigaard, I.A., 2019. Plug and abandonment practices and trends: A British Columbia perspective. Journal of Petroleum Science and Engineering, 106417.

UKCS Decommissioning Cost Report, 2017. Oil & Gas Authority UKCS Decommissioning, 2017 Cost Estimate Report. Oil & Gas Authority, London, United Kingdom.

Vielstädte, L., Haeckel, M., Karstens, J., Linke, P., Schmidt, M., Steinle, L., Wallmann, K., 2017. Shallow gas migration along hydrocarbon wells–An unconsidered, anthropogenic source of biogenic methane in the North Sea. Environmental Science & Technology 51 (17), 10262–10268.

Vielstädte, L., Karstens, J., Haeckel, M., Schmidt, M., Linke, P., Reimann, S., ... Wallmann, K., 2015. Quantification of methane emissions at abandoned gas wells in the Central North Sea. Marine and Petroleum Geology 68, 848–860.

Vielstädte, L., Linke, P., Schmidt, M., Sommer, S., Haeckel, M., Braack, M., Wallmann, K., 2019. Footprint and detectability of a well leaking CO2 in the Central North Sea: Implications from a field experiment and numerical modelling. International Journal of Greenhouse Gas Control 84, 190–203.

Vrålstad, T., Saasen, A., Fjær, E., Øia, T., Ytrehus, J.D., Khalifeh, M., 2019. Plug & abandonment of offshore wells: Ensuring long-term well integrity and cost-efficiency. Journal of Petroleum Science and Engineering 173, 478–491.

Ward, N.I., Alves, T.M., Blenkinsop, T.G., 2016. Reservoir leakage along concentric faults in the Southern North Sea: Implications for the deployment of CCS and EOR techniques. Tectonophysics 690, 97–116.

Well Decommissioning Guidelines, 2018. The UK Oil and Gas Industry Association Limited trading as Oil & Gas UK Guidelines for Well Decommissioning (Issue 6). Oil & Gas UK, Aberdeen, United Kingdom ISBN: 903 004 92 6.

Whitaker, S., 1986. Flow in porous media I: A theoretical derivation of Darcy's law. Transport in Porous Media 1 (1), 3–25.

White, J.E., 1975. Computed seismic speeds and attenuation in rocks with partial gas saturation. Geophysics 40 (2), 224–232. https://doi.org/10.1190/1.1440520.